

# MPPT DESIGN USING GREY WOLF OPTIMIZATION DIFFERENTIAL EVOLUTION (GWODE) TECHNIQUE FOR PARTIALLY SHADED PV SYSTEM

K.GIRINATH BABU, Assistant professor GNITC <sup>(1)</sup>, K.RATNA KISHORI, Assistant professor GNITC <sup>(2)</sup>

**Abstract-**This paper presents a maximum power point tracking (MPPT) design for a photovoltaic (PV) system using a grey wolf optimization differential evolution (GWODE) technique. This “WODE” technique is used for quick and oscillation-free tracking of the global best peak position in a few steps. The unique advantage of this algorithm for maximum power point tracking in partially shaded condition is as, it is free from common and generalized problems of other evolutionary techniques, like longer convergence duration, a large number of search particles, steady-state oscillation, heavy computational burden, etc., This hybrid algorithm is tested in MATLAB simulation and verified on a developed hard-ware of the solar PV system, which consists of multiple peaks in voltage-power curve. . The satisfactory steady-state and dynamic performances of the new hybrid technique under variable irradiance and temperature levels show the superiority over the state-of-the-art control methods.

**Index Terms:** maximum power point tracking (MPPT), partial shading, solar PV, grey wolf optimization differential evolution (GWODE)

## I. INTRODUCTION

Because of pollution and energy crisis the world has a single option, ‘understand and give emphasis to the renewable energy sources’. the solar photovoltaic (PV) and the wind energy sources have proven to be a good and easy solution on the large scale. The new technologies, new topologies, advanced devices, novel control strategies and good management systems are contributing to the success of these renewable energy sources.

Due to static, quiet and movement free characteristic, solar PV system is very popular, reliable and comfortable for users

Therefore, it is highly desirable and to motivate to work with the maximum possible efficiency. Now, the PV power generation system is also commercialized for bulk power in grid-connected mode [2]. Therefore, huge numbers of market players are taking interest and establishing farms (PV Parks), and for maximizing the profit. All are trying to extract maximum power from the PV array or trying to run on the maximum power point (MPP). The MPP tracking (MPPT) is the process through which, the system runs and supplies maximum power to the load. However, the relation between voltage, current and power of the PV system is highly non-linear [2], so to track the MPP needs MPPT algorithms. The basics of the MPPT are based on the current and voltage of the solar PV array. First of all, the current and volt-age of PV array are sensed, then it calculates the instantaneous power, and after that by using an MPPT algorithm, it chooses a duty cycle or voltage reference for the converter, for matching the instantaneous power to the MPP

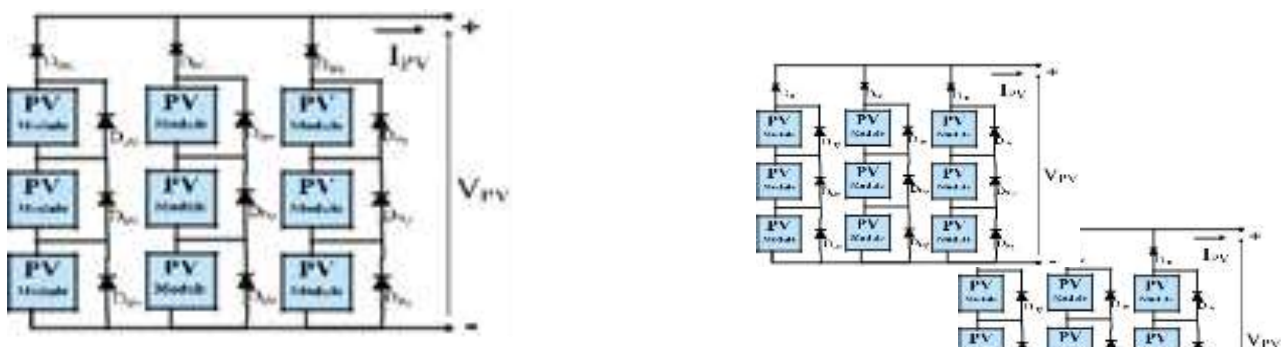


**Fig. 1. PV Array Configuration.**

The structure of a solar PV panel is the series and parallel combination of several modules, as shown in Fig. 1. The volt-age and current ratings of the module are very less. Therefore, for achieving a certain range of output voltage, it needs to add a certain

number of modules in series and the output of each module is bypassed from another module through a bypass diode. Similarly, for a certain range of output current, it needs to add a certain number of series of modules in parallel and the output of each series of the module is prevented from circulating current through blocking diode. This combined system is known as a PV array. When the solar irradiance on all modules are same, then the power- voltage (P-V) curve of the PV array consists of a single peak, but the solar irradiance on all modules are not uniform, then the P-V curve of a PV array consists of multiple peaks and this situation is known as a partially shaded condition [3], [4]. In a practical situation, this non-uniformity of solar irradiance on some module or on the some PV arrays of the PV park arises due to a shadow of clouds, tall buildings, trees etc. The pattern of the shadow decides the pattern of the P-V curve. This pattern of the P-V curve is divided into two types in a dynamic condition.

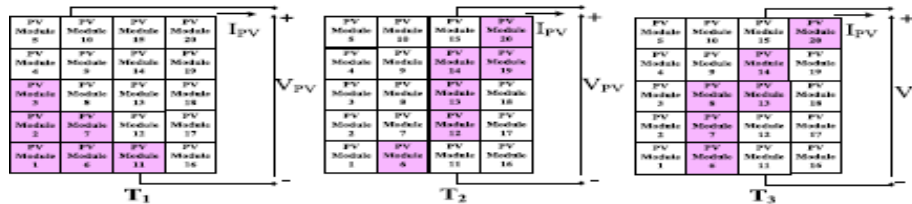


Fig.2 Shading pattern based on CSPSF at a different time instant

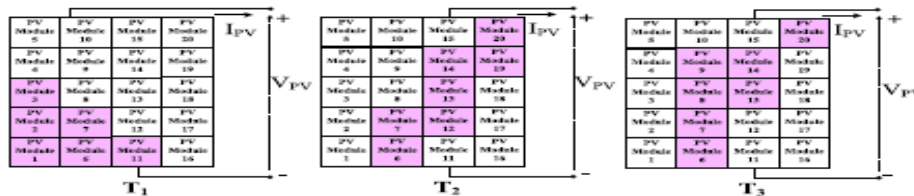


Fig.3 Shading pattern based on CSPDF at a different time instant

**1. Change in shadow pattern, in a similar fashion (CSPSF) at each instant of time:** It means, the number of peaks and the pattern shape of the curve are similar with different magnitude at different solar irradiance. This type of situation arises when the area occupied by the shadow (number of the shaded modules) and sequence in each string are constant as well as the rate of change of the intensity of the shaded region is same with the unshaded region. An example of CSPSF is shown in Fig. 2.

In Fig. 2, at  $T_1$ , the total number of shaded modules are 6, and the sequence is 3 in string 1, 2 in string 2 and 1 in string 3. Moreover, at  $T_2$ , the total number of shaded modules are 6, and sequence is 1 in string 2, 3 in string 3 and 2 in string 4, as well as at  $T_3$ , the total number of shaded modules are 6, and sequence is 3 in string 2, 2 in string 3 and 1 in string 4. Therefore, at  $T_1$ ,  $T_2$  and  $T_3$  the number of peaks and shape of the pattern are same.

**2. Change in shadow pattern, in a different fashion (CSPDF) at each instant of time:** It means, the number of peaks and the pattern shape of the curve are variable in nature with different magnitude at different solar irradiance. This type of situation arises when the area occupied by the shadow (number of the shaded modules) or sequence in each string are not constant as well as the rate of change of the intensity of the shaded region is different with the unshaded region. An example of CSPDF is shown in Fig. 3. In Fig. 3, at  $T_1$ , the total number of shaded modules are 6, and the sequence is 3 in string 1, 2 in string 2 and 1 in string 3. Moreover, at  $T_2$ , the total number of shaded modules are 7, and sequence is 2 in string 2, 3 in string 3 and 2 in string 4, as well as at  $T_3$ , the total number of shaded modules are 7, and sequence is 4 in string 2, 2 in string 3 and 1 in string 4.

Here, at  $T_1$  and  $T_2$ , the total number of shaded modules are not same. However, at  $T_2$  and  $T_3$ , the total number of shaded modules are same, but the sequence is not same. In  $T_2$ , one string contains 3 shaded modules but in  $T_3$ , no string contains 3 shaded modules, similarly, in  $T_3$ , one string contains 4 shaded modules but in  $T_2$ , no string contains 4 shaded modules. Therefore, at  $T_1$ ,  $T_2$  and  $T_3$  the number of peaks and shape of the pattern are not same.

The global maximum power point (GMPP) tracking in the dynamic condition of the partially shaded PV system is a very difficult task. A literature review on solar PV array MPPT reveals that various traditional methods and soft computing techniques have been employed for tracking the GMPP, such as ‘perturb and observe (P&O)’ [5], [6], ‘incremental conductance [7], [8]’, and ‘Hill Climbing [9]’. These are highly suitable for tracking the MPP, but the limitation is, only in uniform or without partially shaded condition. In the case of partial shaded condition, these techniques are not able to differentiate the difference between LMPP and GMPP, so stagnated at first peak, that is LMPP or GMPP, doesn’t matter. Moreover, due to this the enormous amount of power loss occurs, because the GMPP exists at only a single point. Therefore, for searching the GMPP the researchers have proposed ‘fuzzy logic [10]’ and ‘neural net-work [11]’ based control [12], but the ‘excessive storage burden on the processor’, a new type of problem comes in the picture. Because, in fuzzy logic control for fuzzification and de fuzzification, as well as in neural network for training, a huge number of data are required. Therefore researchers tend towards evolutionary algorithms. Due to a simple structure and easy implementation, particle swarm optimization (PSO) [13] is employed for GMPP tracking. In standard PSO [13], the convergence occurs after a large number of iteration, which is the problem, due to high-velocity update or acceleration. Low acceleration follows the smooth trajectory but convergence speed is slow. A high acceleration leads or deviates from the trajectory and moves towards infinity. Thus, more numbers of iterations are conducted to bring the results in the optimum region. In view of these difficulties, some researchers have modified the classical PSO, which is called adaptive perceptive PSO (APPSO) [14], modified PSO [15], [16]. This modification improves the performance, by providing the separate search space to all particles. However, it requires huge numbers of particles for covering the entire region, which creates

complexity and additional computational burden on the processor. For further improvement, an improved PSO (IPSO) [17], novel PSO [18], P&O with PSO [19], differential evolution (DE) with PSO (DEPSO) [20], *etc* are proposed. These algorithms are the combination of PSO and direct updating process. The direct updating process updates the duty cycle according to the ratio of, the change in power and the change in duty cycle. This modification improves the performance in terms of searching ability, but initially, it creates huge oscillations due to large random search. Moreover, these things are repeated again and again on every instant of insolation change in dynamic condition, which makes system oscillatory and unstable. Apart from PSO, firefly algorithm [21], numerical approach [22], and simulated annealing [23], [24] have also used for GMPP tracking. Here, overall performance and searching ability have improved but not significantly.

Therefore, for enhancing the searching ability with less oscillatory and computational burden, Mirjalili *et al.* [25] have developed a grey wolf optimization (GWO) and Mohanty *et al.* [4] have proposed GWO based MPPT algorithm. Grey wolf hunting behavior is based on tracking, encircling and attacking the prey. Since here, tracking process is decided by the linear variable, so encircling and attacking the prey is very similar to the local search behavior [26]. Diverge from the current prey and search a better and better prey is the behavior of global search. Therefore, sometimes, where the difference between GMPP and local MPPT (LMPP) is very less or GMPP is on a very sharp point, in that condition GWO confuses and falls or stagnates on the LMPP (which is very closer to the GMPP).

Therefore, Mirjalili *et al.* [27] again have proposed a ‘Whale optimization (WO)’ algorithm. Which is free from stagnating on the LMPP (which is extremely closer to the GMPP) problem. Moreover, this WO algorithm has proved to be the best technique for nonlinear objective function [27]. This WO algorithm is inspired by the bubble-net hunting strategy of the humpback whale. The trajectory path of the bubble-net attack mechanism of the WO is based on shrinking circling mechanism on the spiral track. In this mechanism, WO starts searching from the outer boundary of the search space and moving on the spiral path with shrinking circling mechanism, so it covers total search space. Since it covers total search space, so the probability of hitting the global best solution is extremely high. In WO algorithm (WOA), the motion of the whale is described in two parts: in a linear direction (for shrinking) with 50% probability and in circled spiral direction with 50% probability [27]. This probability is chosen or decided by a random number. Therefore, the granted probability for hit the global best target is equal to or more than 50%, due to the circled spiral motion of the whale and the probability of fall or stagnate on the LMPP is still equal to or less than 50%, due to local search based linear motion, similar to GWO algorithm. The provision for removal of this problem is also given in this algorithm, which is by increasing the number of the searching whale, but for hardware based on-line running system, where the dynamics are changing at every instant of time, it cannot permit large searching agents. Due to this, it creates initial oscillations, power loss, and computational burden.

In this paper, a new meta-heuristic algorithm is proposed to mitigate the excessive number of spiraled path (large searching agents) and stagnation on the LMPP problems of WO, by hybridizing ‘WO with differential evolution (DE)’ (WODE). Since, the DE has strong searching and fast moving ability [28], [29], so DE is integrated into series with WO, to pull WOA to jump out of the stagnation on the LMPP problem as well as it reduces the number of the spiral paths or iteration number. The role of the DE in WODE algorithm is, it chooses the three best positions of the whale which is decided by WOA and, through crossing all three data from mutation, crossover and selection process, it decides a single best position of the whale. Therefore, in each iteration WOA gets an extra support by DE, which reduces the size of population and number of iteration. These merits show the hardware suitability of the WODE algorithm for online or hardware-based searching process, as well as it is free from common and generalized problems of the other evolutionary techniques, like longer convergence duration, a large number of search particles, steady state oscillation, large computational burden *etc*, which creates power loss, searching delay and oscillations in output.

Therefore, in this situation, WODE algorithm is the best and an appropriate solution to tracking the GMPP in minimum time duration with less number of searching agents. In this work, these merits of the WODE are demonstrated through simulation

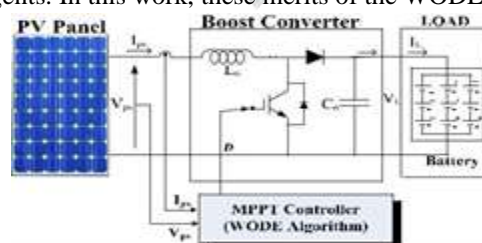


Fig. 4. The operation of Solar PV system with boost converter and load.

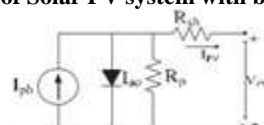


Fig. 5. Circuit Configuration of PV Module.

as well as by hardware results and proven by comparing with the state of the art techniques.

**II. MODELING OF SOLAR PV SYSTEM**

The complete working solar PV model with the load is shown in Fig. 4. Here, the output of the PV panel is supplied to the load (battery charging) through a boost converter. The switching of the boost converter is controlled by WODE.

**A. Modeling of Solar PV (SPV) Module**

For modeling, various techniques are available, but in this work, for simplicity, a single diode model is taken as shown in Fig. 5. The mathematical formulation of the output current ( $I_{pv}$ ) of the PV module is described as [30]

$$I_{pv} = I_{ph} - I_{ao} \left[ e^{\frac{(v_{pv} + R_{sh} I_{pv})q}{N_{cs} k T_c a_{fd}}} - 1 \right] - \frac{v_{pv} + R_{sh} I_{pv}}{R_p}$$

Where,  $I_{ph}$  is the photovoltaic current,  $I_{ao}$  is cell reverse saturation current or diode leakage current,  $V_{pv}$  are the module output voltage,  $R_{sh}$  (0.221Ω) and  $R_p$  (415.5Ω) are equivalent series and parallel resistance,  $N_{cs}$  is the number of series cells,  $q$  is the charge (of an electron) [ $1.60217646 \times 10^{-19}$  C], the Boltzmann constant is  $k$  [ $1.3806503 \times 10^{-23}$  J/K], temperature of the cell's is  $T_c$ ,  $a_{fd}$  is ideality factor of the diode (in general its value is 1 a 1.5) [30].

The mathematical details of  $I_{ph}$  and  $I_{ao}$  are escribed as,

$$I_{ph} = \left( \frac{R_p + R_{sh}}{R_p} I_{sc} + k_i (T_c - T_{ref}) \right) \frac{S}{S_{ref}}$$

$$I_{ao} = \frac{I_{sc} + k_i (T_c - T_{ref})}{e^{\frac{(v_{pv} + R_{sh} I_{pv})q}{N_{cs} k T_c a_{fd}} - 1}}$$

Where,  $I_{sc}$  and  $V_{oc}$  are short circuit current and open circuit voltage.  $K_i$  and  $K_v$  are coefficient of current (0.0032A/K) and voltage (-0.123V/K).  $T_c$  and  $T_{ref}$  are cell's working and reference temperature (25 °C).  $S$  and  $S_{ref}$  are the working and reference irradiation (1000) [30], respectively.



**Fig. 6. Bubble-net with shrink circled spiral motion of whale in WODE.**

**B. Solar PV System Under Partial Shading Condition**

Due to the shadows by clouds, trees or tall buildings, a non-uniformity in the insolation arises on the PV panel. In this situation, some modules receive direct irradiance and some are under partially shaded. The partially shaded modules generate less amount of current in comparisons to other modules. All modules in PV array are in series, so the current through the parallel resistance of partially shaded modules, leads to a voltage drop. This drop reduces the maximum output power and creates hotspots. This problem can be resolved by bypassing currents of all modules through a bypass diode.

In the case of parallel connections of the string, the shaded string withdraws current from rest of the parallel connected strings. This circulating current reduces the efficiency of the PV panel. This problem can be resolved by using a blocking diode ( $D_{BL}$ ). The arrangement of bypass diode ( $D_{By}$ ) and block-ing diode ( $D_{BL}$ ) in a series-parallel combination of modules is shown in Fig. 1.

**III . WODE ALGORITHM AND ITS APPLICATION**

The WODE algorithm is the hybrid of whale optimization (WO) and differential evolution (DE). WO searches the global best very efficiently and DE enhances the performance of the WO, by providing the best start point in each iteration, which enhances the searching ability, reduces the population size and globally maximizes the objective function. The objective function ( $f$ ) is defined as,

$$f(D) = \max PPV(D) \tag{4}$$

$$PPV(D) = VPV(D) \times IPV(D) \quad (5)$$

Where,

PP(D), VPV(D) and IPV(D) are instantaneous power, voltage and current at duty cycle D.

The constraint is described as,  $0 \leq D \leq 1$ .

#### A. Whale Optimization

The WO algorithm is based on hunting method of a hump back whale. This hunting behavior is based on bubble-net feeding mechanism with shrink circled spiral motion [27]. That is shown in Fig. 6

The hunting of a prey is based on three processes,

- 1) Searching, 2) Encircling and 3) Bubble-net attack on the prey.

**1) Searching for Prey:** At initial position, humpback whales start searching randomly (according to initial position). After that, WOA forces to search on a global level by using a random coefficient vector (A). When  $|A| > 1$ , humpback whales start searching in the entire region. This is mathematically described as,

$$D_{ij}(G+1) = D_{rand} - A * d_{ij} \quad (6)$$

Where,  $D_{rand}$  is random duty cycle,  $D_{ij}(G+1)$  is duty cycle for G+1th iteration,  $d_{ij}$  is a coefficient vector of jth whale and ith agent of DE. These,  $d_{ij}$  and A are calculated as,

$$d_{ij} = /C * D_{rand} - D_{ij}(G) / \quad (7)$$

$$A = 2 * \alpha * rand - \alpha \quad (8)$$

Where, 'rand' is a random number between 0 and 1. C is also a random number, which is defined as  $C = 2 * rand$ . ' $\alpha$ ' is linear iteration dependent number, which is defined as,

$$\alpha = 2 - 2(G/g);$$

Where, G is current iteration number and g is a maximum number of iteration.

**2) Encircling the Prey:** In this step, humpback whale recognizes the prey and starts encircling. During encircling, the whale updates its position towards the global best prey. This action takes place when  $|A| < 1$ . Mathematical description of it is as follows,

$$D_{ij} = /C * D_{best}(G) - D_{ij}(G) / \quad (10)$$

$$D_{ij}(G+1) = D_{best} - A * d_{ij} \quad (11)$$

$D_{best}(G)$  is the best duty cycle after  $G_{th}$  iteration

**3) Bubble-Net Attack on the Prey:** During bubble-net attacking mechanism, the motion of the whale is divided into two parts with 50-50% probability: linear motion along the shrinking circle and circular motion along the spiral path [27] as,

$$D_{ij}(G+1) = \begin{cases} D_{best}(G) - A * d_{ij} & \text{if } P_c < 0.5 \\ d'_{ij} * e^{bL} * \cos(2\pi L) + D_{best}(G) & \text{if } P_c \geq 0.5 \end{cases}$$

$$D'_{ij} = |D_{best}(G) - D_{ij}(G)|$$

## B. DIFFERENTIAL EVOLUTION

DE is a probabilistic based global search optimization. In this work, the role of the DE is to enhance the performance of WO. For this purpose, DE selects 3 target vectors ( $D_{i1}(G)$ ,  $D_{i2}(G)$  and  $D_{i3}(G)$ ) from the whale population and passes through the searching process of the DE, which is completed in three steps: mutation, crossover and selection [28].

#### 1) Mutation

DE mutation process generates a trial vector ( $U_i(G)$ ) from the parent vector ( $D_{i1}(G)$ ,  $D_{i2}(G)$  and  $D_{i3}(G)$ ) by using weighted differential coefficients or scale factor of mutation ( $\zeta$ ). This generation process is mathematically described as,

$$U_i(G) = D_{i1}(G) + \zeta * (D_{i2}(G) - D_{i3}(G)) \quad (14)$$

Where, 'i' is the current population number.

#### 2) Crossover

During crossover, DE generates child ( $D_i(G)$ ) from the trial vector ( $U_i(G)$ ) and best parent ( $D_{i1}(G)$ ) of the parents vector by using crossover probability ( $\rho$ ). This process is shown as,

$$\begin{cases} U_i(G) & \text{if } rand > \rho \\ D_{i1}(G) & \text{if } rand \leq \rho \end{cases} \quad (15)$$

$$D'_{ij} = U_i(G) \quad \text{if } \text{rand} \leq \rho$$

Where, 'rand' is a random number between 0 and 1.

### 3) Selection

DE selects the best option ( $D_i(G+1)$ ) for next generation, from the parent and child on the basis of the best value of the fitness function ( $f$ ). The selection process is described as [28],

$$D_i(G+1) = \begin{cases} D_i(G) & \text{if } f(D_i(G)) > f(D_{i1}(G)) \\ D_{i1}(G) & \text{Otherwise} \end{cases} \quad (16)$$

C. **Hybridizing and Application of WODE Algorithm:** WO has very efficient searching and solving ability of nonlinear problem, but it requires a large number of whales or iterations and in some cases, it is stagnated on LMPP (which is extremely closer to the GMPP) due to linear motion of whale during shrinking circle with 50% probability. Moreover, DE has strong comparative studies and optimal location searching or generating ability in defined region. These merits of the DE are very suitable for reducing the number of iteration as well as for forcing to the jump out from the stagnation on LMPP problem by discovering an optimal location for whale at the end of every iteration. In detail, it is discussed in Section I.

The combined effect of both algorithms can be found by hybridizing of both, known as WODE algorithm. Here, DE is integrated into series with WO. Where, WO starts searching on a circular path and at the end of each round of the searching, it passes all information to the DE. DE analyses and finds a single best place and optimal accelerating speed of the whale by using three sets of location information, which is decided by WO. This combined performance reduces the effects of random constants and metaheuristic nature of the algorithm by increasing the convergence speed. Moreover, computational burden and stagnation problems are removed through mutation, crossover, and selection process of the DE. As well as, it drastically reduces the number of iteration, which is shown in Fig. 6. The paths of whale are shown by dark red lines and jump of DE is shown by the black arrow.

The flowchart of the WODE is shown in Fig. 7.

The different stages and steps of the WODE for problem-solving are described as:

- 1st Step;
  - a) Define objective function (by using (4) and (5)),
  - b) Provide algorithm constants ( $b, \rho, \zeta$ ), upper ( $D_U$ ) and lower ( $D_L$ ) limit of the variable at initial stage, initial error constant ( $\epsilon_0$ ) and number of population ( $P_0$ ).
- 2nd Step;
  - a) Set,  $\text{flag} = 1, S_f = 1, D_{\min} = D_L, D_{\max} = D_U, \epsilon = \epsilon_0$
- 3rd Step;
  - a) Randomly create 4 duty cycles (3 for WO and 1 for DE) within upper ( $D_{\max}$ ) and lower ( $D_{\min}$ ) limit,
  - b) Find power for duty cycle of WO,
  - c) By using the  $D_{\max}$  and  $D_{\min}$  find  $P_{\max}$  and  $P_{\min}$ .
- 4th Step;
  - a) Find power for duty cycle of DE,
  - b) According to power choose best 3 duty cycles,
  - c) Find  $D_{\text{best}}$  according to  $P_{\text{best}}$ ,
  - d) Find  $\Delta P (= P_i - P_{i-1})$  for selected all 3 duty cycles.
- 5th Step;
  - Check,  $P$  is in between  $[P_{\max}, P_{\min}]$ ?
  - a) If, yes, go to step 6,
  - b) If, no, go to step 2.
- 6th Step;
  - Check,  $P$  is less than  $\epsilon$ ?
  - a) If, yes, go to step 7,
 If, no, go to step 8
- 7th Step;
  - a)  $\text{flag} = \text{flag} + 1$ ,
  - b)  $S_f = S_f / \text{flag}$
  - c)  $D_{\min} = (1 - S_f) * D_{\text{best}}$
  - d)  $D_{\max} = (1 + S_f) * D_{\text{best}}$
  - e)  $E = S_f * E_0$ ,
  - f) Go to step 3.
- 8th Step; Pass all 3 duty cycles from WO.
  - a) Search for prey (by using (6)–(9)),

- b) Encircle the prey (by using (10) and (11)),
- c) Bubble-net attack on the prey (by using (12) and (13)).
- 9th Step;
- a) Find power for all duty cycle and arrange in descending order.
- 10th Step; Pass all 3 duty cycle from DE.
- a) Mutation (by using (14)),
- b) Crossover (by using (15)),
- c) Selection (by using (16)).
- 11th Step; Update duty cycle and go to step 4

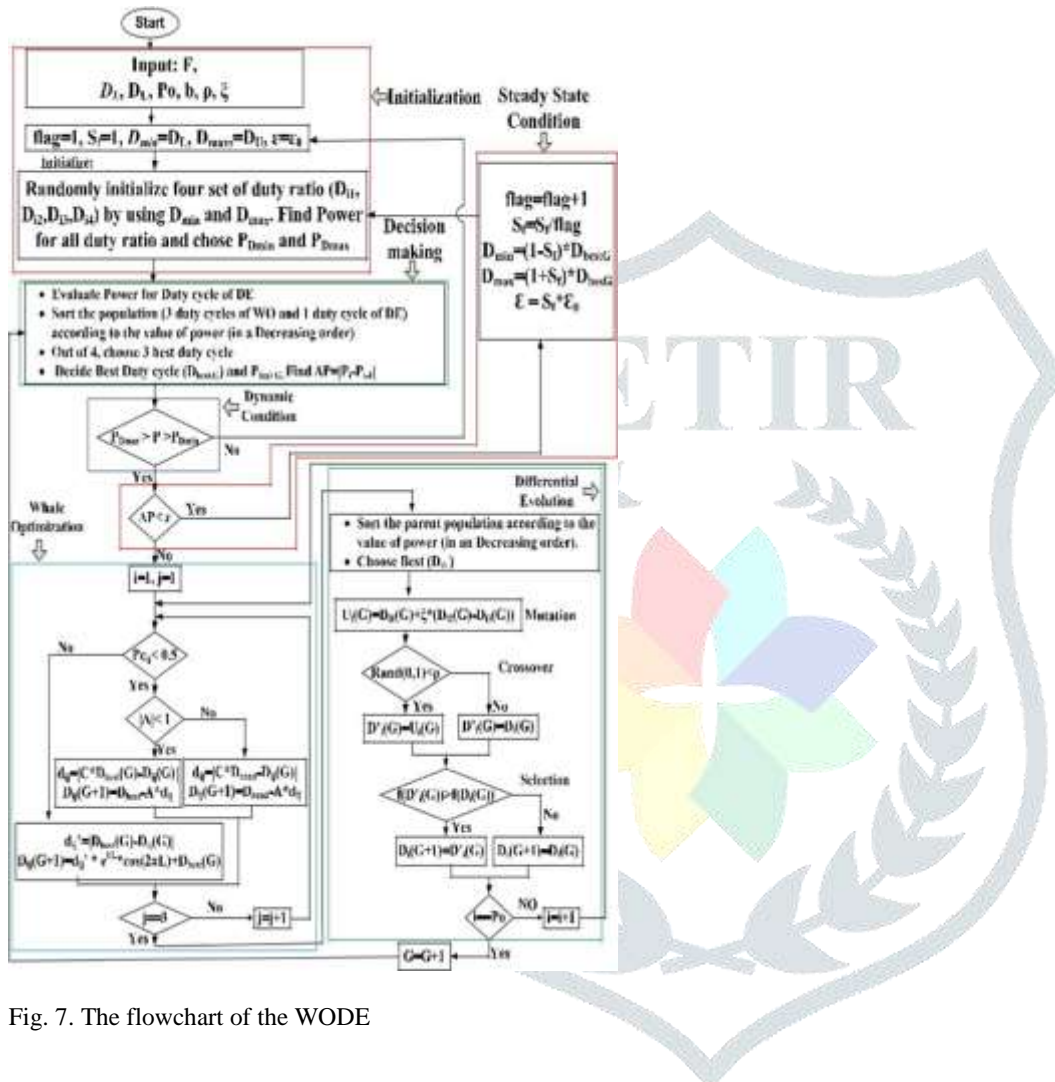


Fig. 7. The flowchart of the WODE

This is an online process, so the cyclic process is repeated again and again. The uniqueness of this process is, at the end of every iteration, the performance of all whales are summarized and, a best place for a starting the new iteration is decided. An-other best part is, it has extremely less steady state oscillation and quick dynamic performance. The steady state oscillation is controlled by ‘step 7’, which exponentially reduces the os-cillation in every iteration. Moreover, the dynamic condition is sensed by ‘step 5’ and controlled by ‘step 7’. Here the pop-ulation size is only 4. Therefore, the small population, quick dynamic performance and negligible steady state oscillations enhance the searching ability tremendously, as well as the com-putational burden is very less so, it can be easily implemented on a cheap microcontroller

**D. Selection of Control Parameters**

The control parameters are the key of every algorithm, be-cause the performance of the algorithm is directly influenced by the control parameters. In WODE, the control variables are, shape constant of the logarithmic spiral (b), scaling factor (zeta) and crossover probability (rho).

1) **Shape Constant of the Logarithmic Spiral (b):** This ‘b’ defines the shape and radius of the spiral net in WO. In general, a small value is taking for ‘b’, so its accuracy level improves. However, a very small value, decreases the convergence rate [27]. Therefore, it takes an optimum value for ‘b’ in the range of [0.1, 1].

2) **Scaling Factor ( $\zeta$ ):** This ' $\zeta$ ' controls the amplification of the differential variations in DE. The smaller value of  $\zeta$ , reduces the differential variations but, it takes a long time to converge and larger value facilitates exploration. But it may lead to overshoot optimum results [28], [29]. Therefore, the optimum range is [0, 5], 5 is the maximum range, because in MPPT problem, more than 5 times differential variations amplification, abruptly enhances the values, and it goes beyond the range ( $>1$ ).

**Crossover Probability ( $\rho$ ):** Crossover probability ( $\rho$ ) is also known as recombination probability. It directly influences the diversity of DE. It's higher value increases diversity, exploration and convergence rate, but the search robustness decreases. The search robustness enhances in the case of small  $\rho$  but convergence rate becomes very low [28], [29]. Therefore, the optimum range of  $\rho$  is [0.1, 1]

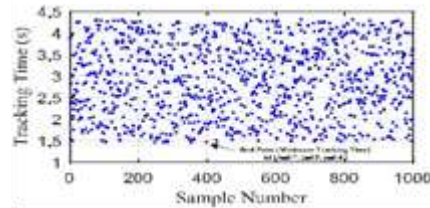


Fig. 8. GMPP tracking time at different combinations of constant in 1st step.

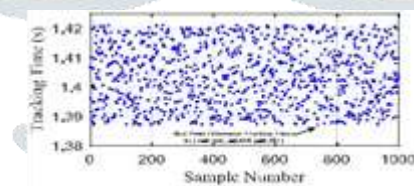


Fig. 9. GMPP tracking time at different combinations of constant in 2nd step.

Here, the main challenge is, to choose one set of value from the range. So that the result is globally and universally best. This selection process is completed in two steps,

Step 1st; The optimum range of all constants ( $b \in [0.1, 1]$ ,  $\zeta \in [0, 5]$  and  $\rho \in [0.1, 1]$ ) are divided into 10 parts, and samples are created by using different combinations. The total number of combinations are 1000 ( $10^3$ ). Here, most critical and complicated case (on pattern-4) is selected for testing, and the simulation is run 20 times by using each combination of constant as well as the average tracking time is calculated for all combination. The solution of the 1st step is, the combination, at which the average tracking time is minimum. The plot of all average tracking time w.r.t. the sample is shown in Fig. 8.

Fig. 8 shows that, the tracking time is varying from 1.451 s to 4.319 s. and the best set of constant values are  $b = 0.7$ ,  $\zeta = 0.5$ , and  $\rho = 0.4$  for 1.451 s.

Step 2nd; The solution of 1st step, varies  $\pm 10\%$  and separate range for all constants ( $b \in [0.63, 0.77]$ ,  $\zeta \in [0.45, 0.55]$  and  $\rho \in [0.36, 0.44]$ ) are made. Again range is divided into 10 parts and samples are created using different combinations. By using each combination, the simulation is again run by 20 times and the average tracking time is calculated for all combination. The solution of the 2nd step is the combination at which, the average tracking time is minimum. The plot of all average tracking times w.r.t. the sample is shown in Fig. 9.

Fig. 9 reveals that, the tracking time is varying from 1.387 s to 1.421 s and the best set of constant values are  $b = 0.754$ ,  $\zeta = 0.494$ , and  $\rho = 0.387$  for 1.387 s. Here, the variation between best and worst result is less (34ms), so the result of the 2nd step can be taken for global use.

However, if the results of the 2nd step are not suitable (gap between best and worst is more), then again step 2 is repeated, by using the result of 2nd step.

#### IV. RESULTS AND DISCUSSION

The performance evaluation of the proposed WODE method is performed over the 'SPV fed battery load by using a boost converter', which is shown in Fig. 4. Here, variations in solar insolation and temperature, both are considered, which pattern

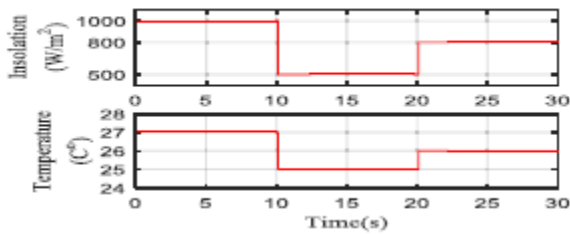


Fig. 10. The pattern of insolation and temperature variation.

TABLE-I  
CONSTANTS OF ALL ALGORITHMS

Algorithm	WODE	GWO	IPSO
Algorithm parameters	$\zeta = 0.494$ ,	' $\alpha$ ', linearly decrement from 2 to 0	$C1,max = 2,$ $C2,max = 2,$ $C1,min = 1, C2,min = 1,$ $Wmax = 1, Wmin = 0.1$
Parameters	$\rho = 0.387,$ $b = 0.754$		

TABLE-II  
CIRCUIT PERAMETERS

Circuit parameter	Selected Value
Inductor of boost converter (L <sub>o</sub> )	3.5 mH
Commutation frequency of boost converter	20 kHz
DC bus capacitor (C <sub>o</sub> )	500 $\mu$ F
dSpace functional frequency	50 kHz
Mode of operation	Continuou s

TABLE III

DESCRIPTION OF ALL PATTERN

Pattern	Number of peaks	GMPP Location	LMPP Peaks
Pattern-1	3	First (1st peak)	2nd and 3rd
Pattern-2	5	Middle (4th peak)	1st, 2nd, 3rd and 5th
Pattern-3	4	Last (4th peak)	1st, 2nd and 3rd

is shown in Fig. 10. Its superiority is proven through comparison with the most recent technique 'GWO' [4] and highly popular 'IPSO' [11] algorithm. The algorithm parameters of all tech-niques are given in Table I. Moreover, the circuit parameters are given in Table II.

**A. Change in Shadow Pattern, in a Similar Fashion (CSPSF) at Each Instant of Time**

To verify the effectiveness of all techniques in CSPSF situ-ation, 3 types of PV curve patterns are taken for simulation as well as during hardware implementation. The detail description of all patterns is given in Table III.

1) *Simulation Results:* The performance of the SPV system is simulated by using MATLAB 2010a software on Dell computer with Intel core i3, 2.4 GHz processor, 2 GB of RAM memory and windows 7 operating system. For simulation, a PV array of  $V_{oc} = 480$  V,  $I_{sc} = 11.26$  A,  $P_{m,pp} = 4$  kW at  $25^{\circ}\text{C}$  with irradiation  $1000$   $\text{W}/\text{m}^2$  in without shaded condition, and as a load, the battery bank of  $480$  V is considered. More-over, in each pattern, the change in dynamics on every  $10$  s, according to Fig. 10 is considered and 3D representation of PV characteristic or all patterns are shown in Fig. 11.

The simulations for all 3 patterns by WODE, GWO and IPSO methods are performed in similar circuit conditions and results

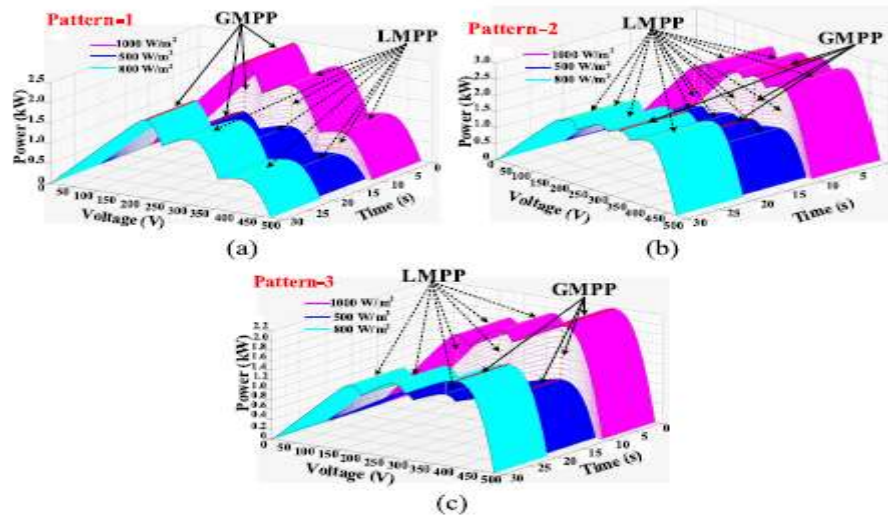


Fig.11 P-V-T Curves of (a) Pattern-1(b) Pattern-2(c) Pattern-3

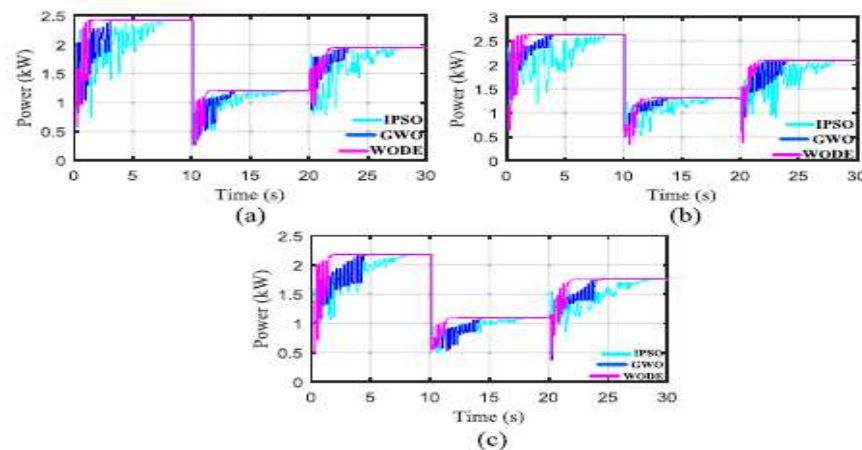


Fig.12 power wave forms of (a) Pattern-1(b) Pattern-2(c) Pattern-3

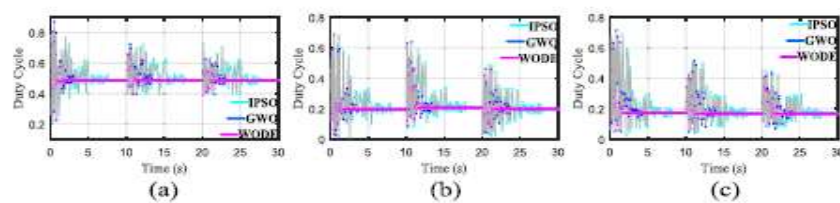


Fig 13 Duty cycle of (a) pattern-1(b) Pattern-(c)pattern-3

are plotted over each other for detail comparative study. The power and duty cycle waveforms for pattern 1 are shown in Fig. 12(a) and Fig. 13(a) respectively. Similarly, for pattern 2 and pattern 3, the waveforms are shown in Fig. 12(b), Fig. 13(b), and in Fig. 12(c), Fig. 13(c), respectively. Moreover, all results are summarized in Table IV.

From all waveforms and Table IV, it can be seen clearly, the WODE is tracking the GMPP very quickly and efficiently, on all patterns. During pattern-1, the average GMPP tracking times of the IPSO and GWO are  $7.673$  s and  $3.016$  s. However, the WODE is taking only  $1.296$  s to reach the GMPP. Similarly, on pattern-2 and pattern-3, IPSO is taking  $8.01$  s and  $7.93$  s

TABLE IV  
Simulation Result of All Methods

Time Interval →		Time taken for tracking the GMPP			Overall % Tracking Efficiency (in 30s time span)
		6-10s (800W/m <sup>2</sup> - 1000W/m <sup>2</sup> )	10s-20s (1000W/m <sup>2</sup> - 500W/m <sup>2</sup> )	20s-30s (500W/m <sup>2</sup> - 800W/m <sup>2</sup> )	
Pattern-1 ( $P_{mpp}=2450.8W$ )	IPSO	7.46s	7.89s	7.67s	87.683
	GWO	2.98s	3.12s	2.95s	95.633
	<b>WODE</b>	<b>1.27s</b>	<b>1.23s</b>	<b>1.39s</b>	<b>98.968</b>
Pattern-2 ( $P_{mpp}=2637.28W$ )	IPSO	8.23s	7.81s	7.99s	85.053
	GWO	3.48s	3.16s	3.59s	94.254
	<b>WODE</b>	<b>1.53s</b>	<b>1.41s</b>	<b>1.33s</b>	<b>98.473</b>
Pattern-3 ( $P_{mpp}=2179.72W$ )	IPSO	8.13s	7.95s	7.73s	89.115
	GWO	4.12s	3.87s	3.77s	95.613
	<b>WODE</b>	<b>1.38s</b>	<b>1.29s</b>	<b>1.42s</b>	<b>99.091</b>

as well as GWO is taking 3.416 s and 3.92 s but WODE is taking only 1.423 s and 1.363 s to reach the GMPP. It means, on an average, WODE is more than 2 times faster w.r.t. GWO and more than 5 times faster w.r.t. IPSO. Moreover, the overall efficiency of the WODE is also better w.r.t. GWO and IPSO algorithm.

2) *Hardware Implementation:* A solar PV array simulator (AMETEK ETS600x17DPVF) is used to generate the required P-V and I-V characteristics. The power of the SPV simulator is supplied to the load (battery) by using a boost converter. The Hall Effect current (LA-55p) and voltage (LV-25) sensors are used for sensing the voltage and current signal of the SPV array. The out-puts of the sensors are given to the 'Analog to Digital converter (ADC)' of the 'Digital Signal Processor (dSpace MicroLab-Box)' board. The processor is used for executing the MPPT al-

gorithms and generating the PWM signals for the power switch of the boost converter. Moreover, the signals ( $P_{pv}$ ,  $I_{pv}$ ,  $V_{pv}$ ) are obtained from the DSP-dSpace and displayed on DSO. The photograph of the hardware prototype is shown in Fig. 14.

Here, the solar panel rating, shading pattern, load, solar inso-lation and temperature variation, all are same, which have been used during simulation.

The steady state response and achieved % MPPT on patterns-1, 2 and 3 at 1000 W/m<sup>2</sup> irradiation by IPSO, GWO and WODE are shown in Fig. 15, Fig. 16 and Fig. 17, respectively, as well as in summarized form are shown in Table V. These figures and Table V reveal that, the steady state performance of the WODE is good in each case w.r.t. IPSO and GWO. The achieved %MPPT is highlighted by the red boundary on every figure. These figures also show the information about the rating of  $P_{mpp}$ ,  $V_{mpp}$ ,  $I_{mpp}$  and error in  $V_{mpp}$  and  $I_{mpp}$ . Moreover, the obtained experimental results for Pattern-2 by IPSO, GWO and WODE algorithm are shown in Fig. 18. The experimental results

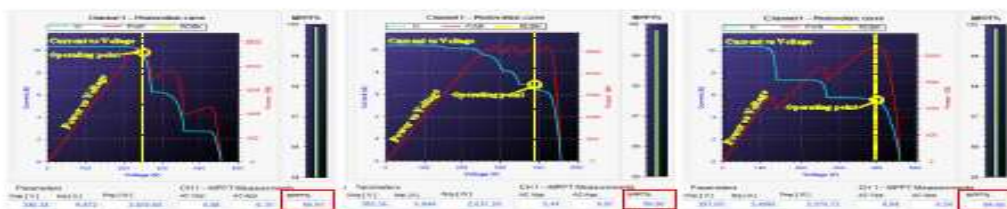


Fig. 15. Achieved % MPPT in Steady state on pattern-1, 2 and 3 by IPSO.

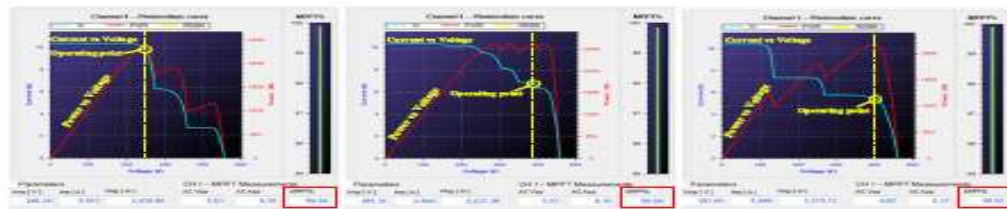


Fig. 16. Achieved % MPPT in Steady state on pattern-1, 2 and 3 by GWO.

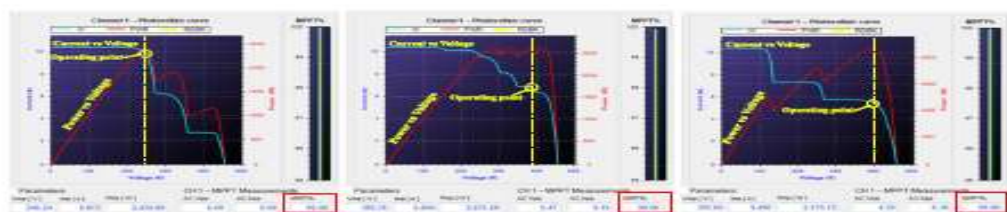


Fig. 17. Achieved % MPPT in Steady state on pattern-1, 2 and 3 by WODE.

TABLE V

THE STEADY STATE RESPONSE

The steady state response	Error in $V_{mppt}$	Error in $I_{mppt}$	Achieved % MPPT	
<b>Pattern-1</b> • $P_{mppt}=2430.8W$ • $V_{mppt}=246.24V$ • $I_{mppt}=9.872 A$	IPSO	6.88 V	0.31 A	99.91%
	GWO	5.83 V	0.25 A	99.94%
	<b>WODE</b>	<b>6.00 V</b>	<b>0.08 A</b>	<b>99.98%</b>
<b>Pattern-2</b> • $P_{mppt}=2637.28W$ • $V_{mppt}=385.36 V$ • $I_{mppt}=6.844 A$	IPSO	5.41 V	0.97 A	99.80%
	GWO	5.53 V	0.76 A	99.84%
	<b>WODE</b>	<b>5.47 V</b>	<b>0.19 A</b>	<b>99.96%</b>
<b>Pattern-3</b> • $P_{mppt}=2179.72W$ • $V_{mppt}=397.05 V$ • $I_{mppt}=5.490 A$	IPSO	4.04 V	0.54 A	99.90%
	GWO	4.82 V	0.37 A	99.92%
	<b>WODE</b>	<b>4.30 V</b>	<b>0.10 A</b>	<b>99.98%</b>

TABLE VI

HARDWARE RESULTS OF ALL METHODS

Time Interval →		Time taken for tracking the GMPP		
		0-10s (800W/m <sup>2</sup> - 1000W/m <sup>2</sup> )	10s-20s (1000W/m <sup>2</sup> - 500W/m <sup>2</sup> )	20s-30s (500W/m <sup>2</sup> - 800W/m <sup>2</sup> )
<b>Pattern-1</b> • $P_{mppt}=2430.8W$ • $V_{mppt}=246.24V$ • $I_{mppt}=9.872 A$	IPSO	7.57s	8.03s	7.84s
	GWO	3.21s	3.24s	3.17s
	<b>WODE</b>	<b>1.43s</b>	<b>1.37s</b>	<b>1.42</b>
<b>Pattern-2</b> • $P_{mppt}=2637.28W$ • $V_{mppt}=385.36 V$ • $I_{mppt}=6.844 A$	IPSO	8.32s	7.97s	8.11s
	GWO	3.57s	3.25s	3.61s
	<b>WODE</b>	<b>1.56s</b>	<b>1.43s</b>	<b>1.35s</b>
<b>Pattern-3</b> • $P_{mppt}=2179.72W$ • $V_{mppt}=397.05 V$ • $I_{mppt}=5.490 A$	IPSO	8.27s	8.08s	7.91s
	GWO	4.31s	3.96s	3.83s
	<b>WODE</b>	<b>1.41s</b>	<b>1.43s</b>	<b>1.58s</b>

for all patterns, achieved by all algorithms, in summarized form are shown in Table VI.

In the experimental results, the time division on the X-axis is 5 s/dev. in Fig. 18. Fig. 18(a) shows the results of IPSO algorithm for pattern-2. Where in dynamic change condition, IPSO takes

7.97 s for insolation change 1000 W/m<sup>2</sup> to 500 W/m<sup>2</sup> and 8.11 s for insolation change 500 W/m<sup>2</sup> to 800 W/m<sup>2</sup> to track the GMPP. In the case of GWO, the performance is slightly improved for both insolation changes, that is shown in Fig. 18(b), it takes 3.25 s and 3.61 s to reach the GMPP. This tracking time is also too much. In this situation, the WODE has performed extremely good and tracked the GMPP only in 1.43 s and 1.35 s, which are shown in Fig. 18(c). These experimental results again show that, the tracking capability of WODE is approximately 5 to 6 times faster from IPSO and 2 to 3 times faster from GWO. Moreover, here, the load voltage is equal to the open-circuit voltage of the PV panel, so the permissible range of duty cycle variation is from 0 to 1. However, the random variation, random motion or oscillation during searching in WODE are very less in comparison to the IPSO and GWO, which can be seen in duty cycle curve in Fig. 18.

**B. Change in Shadow Pattern, in a Different Fashion (CSPDF) at Each Instant of Time**

To verify the effectiveness of all algorithms in CSPDF situation, a very complex PV pattern is taken for simulation as well as during hardware implementation. In this curve, the PV pattern at different insulations are not same, the fashion of PV pattern is changing randomly at different insolation. In the con-sidered waveform, at insolation 1000 W/m<sup>2</sup>, 500 W/m<sup>2</sup> and at 800 W/m<sup>2</sup>, the waveforms are like pattern-3, pattern-2 and pattern-1 respectively. This waveform is considered as pattern-4 and it is shown in Fig. 19.

1) *Simulation Results:* Here, the solar panel rating, load, so-lar insolation and temperature variation, all are same, which have been used in CSPSF. The simulations using WODE, GWO and IPSO methods are performed in a similar circuit and environmental conditions. Moreover, the results are shown in Fig. 20.

The performance during dynamics shows the superiority of WODE over, all another methods. Its average time to reach the GMPP is only 1.34 s, where GWO is taking 3.65 s and IPSO is taking 8.37 s. It means the tracking ability of the WODE is

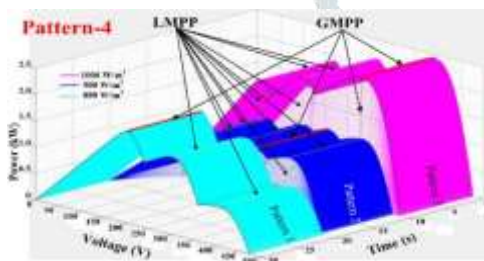


Fig. 19. P-V-T curve of pattern-4.

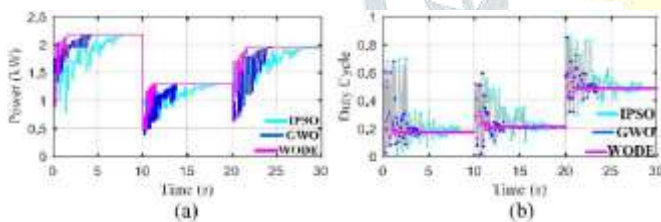


Fig. 20. Simulation Results of Pattern-4, (a) Power and (b) duty cycle.

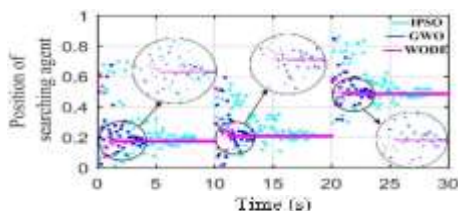
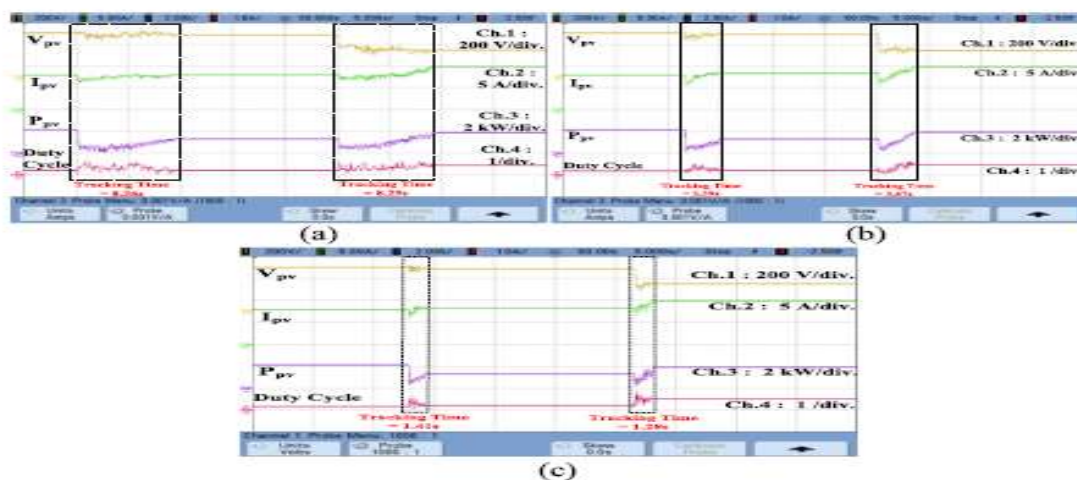


Fig. 21. Convergence graph of all algorithm.

more than 2 times faster in comparison to GWO and more than 6 times faster in comparison to IPSO. Moreover, the efficiency of the WODE is also higher (98.117%) w.r.t. GWO (94.16%) and IPSO (87.021%). In MPPT, the efficiency is directly related to convergence or tracking time. Low tracking time means, fast convergence, less power loss so the efficiency is higher, vice versa. Here, the load voltage is equal to the open-circuit voltage of the PV panel, so the duty cycle can vary from 0 to 1, so for searching an optimum duty cycle, a wide area is available. The convergence of the duty cycle by the different algorithms are shown in Fig. 21, which shows that, in each time interval WODE converges very quickly w.r.t. GWO and IPSO.

2) **Hardware Implementation:** The hardware system is same, which is described previously and shown in Fig. 14. Moreover, the rating of the PV array and circuit configurations is same, which is used in the simulation. Experimental results (voltage, current, power and duty cycle) of the IPSO, GWO, and WODE algorithms are shown in Fig. 22. Moreover, all results in summarized form of pattern-4 are presented in Table VII.

In the experimental results, the time division on the X-axis is 5 s/div. Fig. 22(a) shows the results of IPSO algorithm for pattern-4. Where in dynamic change condition, IPSO takes 8.43 s for insolation change 1000 W/m<sup>2</sup> to 500 W/m<sup>2</sup> and 8.37 s for insolation change 500 W/m<sup>2</sup> to 800 W/m<sup>2</sup> to track the GMPP. In the case of GWO, the performance is comparatively good for both insolation changes; it takes 3.43 s and 3.72 s to reach the GMPP, which is shown in Fig. 22(b). This tracking time interval is also too much, which creates excessive power loss and reduces



Experimental result of (a) IPSO (b) GWO (c) WODE

RESULTS OF ALL METHODS ON PATTERN-4

TABLE VII

Pattern-4	Time taken of all algorithms						
	On Simulation			On Hardware			
<b>Time Schedule</b>	<b>P<sub>mpp</sub></b>	<b>IPSO</b>	<b>GWO</b>	<b>WODE</b>	<b>IPSO</b>	<b>GWO</b>	<b>WODE</b>
0-10 s	2179.72 W	8.46 s	3.88 s	<b>1.33 s</b>	8.51 s	3.93 s	<b>1.37 s</b>
10 s-20 s	1299.86 W	8.36 s	3.39 s	<b>1.41 s</b>	8.43 s	3.43 s	<b>1.47 s</b>
20 s-30 s	1949.45 W	8.29 s	3.67 s	<b>1.28 s</b>	8.37 s	3.72 s	<b>1.31 s</b>

OVERALL PERFORMANCES OF ALL METHODS

TABLE VIII

Case	Methods	CSPSF			CSPDF		
		Average Number of iteration	Average % efficiency	Average tracking time	Average Number of iteration	Average % efficiency	Average tracking time
IPSO	29	87.967	8.01s	31	87.021	8.43s	
GWO	15	95.167	3.57s	17	94.160	3.69s	
<b>WODE</b>	<b>7</b>	<b>98.844</b>	<b>1.36s</b>	<b>9</b>	<b>98.117</b>	<b>1.38s</b>	

the efficiency. Therefore, WODE is the good option, which takes the only 1.47 s for insolation change 1000 W/m<sup>2</sup> to 500 W/m<sup>2</sup> and 1.31 s for insolation change 500 W/m<sup>2</sup> to 800 W/m<sup>2</sup> to track the GMPP, it is shown in Fig. 22(c). It means, on an average, the performance of the WODE is more than 2 times faster in comparison to GWO and more than 6 times faster in comparison to IPSO. Moreover, the random motion or searching duration, in the case of WODE is comparatively very less w.r.t. GWO and IPSO, which can be seen in duty cycle waveform. There-fore, WODE converges quickly. These quick, accurate and free from initial position tracking abilities show the effectiveness of WODE algorithm.

The average tracking time, efficiency and the number of iteration of IPSO, GWO and WODE for CSPSF and CSPDF are shown in Table VIII.

Table VIII reveals that, in each case, on all patterns, the performance of the WODE is very good in terms of tracking time as well as efficiency. The average tracking times of WODE in the case of CSPSF and CFPDF are only 1.36 s and 1.38 s, where GWO is taking 3.57 s and 3.69 s, as well as IPSO is taking 8.01 s and 8.43 s. Similarly, the average efficiency of WODE in the

case of CSPSF and CFPDF is 98.844% and 98.117%, where the efficiency of GWO is 95.167% and 94.16%, as well as the efficiency of IPSO is 87.967% and 87.021% only. The bar chart of achieved tracking time of all 4 patterns by WODE, GWO and IPSO are shown in Fig. 23

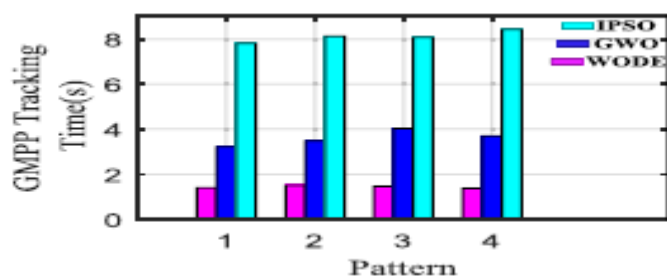


Fig.23.Achieved Tracking time o all patterns

## V.CONCLUSION

A new evolutionary technique called WODE has been pro-posed for MPPT under partial shading condition. This WODE algorithm is the hybrid of WO and DE evolutionary techniques. WO has the strong searching ability in a wide area and DE reduces the effect of random constants and metaheuristic nature by increasing (accelerating) the convergence speed of the algorithm. Therefore, the searching ability of the proposed WODE algorithm is quicker, reliable, system independent and free from the initial condition as well as the computational burden is also very less, for MPPT in all types of weather and shading condition on the PV panel. The performance of the WODE in GMPP tracking under partial shading in steady state and dynamic conditions has been compared to the performance of some recent techniques (GWO and IPSO) in the same irradiance, temperature and hardware condition on high power rating. The simulated and test results of the WODE in both conditions: change in the shadow pattern in a similar fashion and different fashion in a dynamic condition; show the superiority over all existing methods. This proposed method (WODE) can track GMPP very accurately and more than 2 to 5 times faster in comparison to the state of the art methods with a good dynamic as well as steady-state response in every type of environmental condition.

## REFERENCES

- [1] B. Subudhi and R. Pradhan, "A comparative study on maximum power point tracking techniques for photovoltaic power systems," *IEEE Trans. Sustain. Energy*, vol. 4, no. 1, pp. 89–98, Jan. 2013.
- [2] C. Jain and B. Singh, "A three-phase grid tied SPV system with adaptive DC link voltage for cpi voltage variations," *IEEE Trans. Sustain. Energy*, vol. 7, no. 1, pp. 337–344, Jan. 2016.
- [3] H. Patel and V. Agarwal, "Maximum power point tracking scheme for PV systems operating under partially shaded conditions," *IEEE Trans. Ind. Electron.*, vol. 55, no. 4, pp. 1689–1698, Apr. 2008.
- [4] S. Mohanty, B. Subudhi, and P. K. Ray, "A new MPPT design using grey wolf optimization technique for photovoltaic system under par-tial shading conditions," *IEEE Trans. Sustain. Energy*, vol. 7, no. 1, pp. 181–188, Jan. 2016.
- [5] S. K. Kollimalla and M. K. Mishra, "Variable perturbation size adaptive P&O MPPT algorithm for sudden changes in irradiance," *IEEE Trans. Sustain. Energy*, vol. 5, no. 3, pp. 718–728, Jul. 2014.
- [6] M. A. Elgendy, B. Zahawi, and D. J. Atkinson, "Operating characteristics of the P&O algorithm at high perturbation frequencies for standalone PV systems," *IEEE Trans. Energy Convers.*, vol. 30, no. 1, pp. 189–198, Mar. 2015.
- [7] M. A. Elgendy, B. Zahawi, and D. J. Atkinson, "Assessment of the in-cremental conductance maximum power point tracking algorithm," *IEEE Trans. Sustain. Energy*, vol. 4, no. 1, pp. 108–117, Jan. 2013.
- [8] M. A. Elgendy, D. J. Atkinson, and B. Zahawi, "Experimental investigation of the incremental conductance maximum power point tracking algorithm at high perturbation rates," *IET Renewable Power Gener.*, vol. 10, no. 2, pp. 133–139, Feb. 2016.
- [9] B. N. Alajmi, K. H. Ahmed, S. J. Finney, and B. W. Williams, "Fuzzy-logic-control approach of a modified hill-climbing method for maximum power point in microgrid standalone photovoltaic system," *IEEE Trans. Power Electron.*, vol. 26, no. 4, pp. 1022–1030, Apr. 2011.
- [10] R. Guruambeth and R. Ramabadrán, "Fuzzy logic controller for partial shaded photovoltaic array fed modular multilevel converter," *IET Power Electron.*, vol. 9, no. 8, pp. 1694–1702, Jun. 2016.
- [11] Syafaruddin, E. Karatepe, and T. Hiyama, "Artificial neural network-polar coordinated fuzzy controller based maximum power point tracking control under partially shaded conditions," *IET Renewable Power Gener.*, vol. 3, no. 2, pp. 239–253, Jun. 2009.
- [12] A. Chikh and A. Chandra, "An optimal maximum power point tracking algorithm for PV systems with climatic parameters estimation," *IEEE Trans. Sustain. Energy*, vol. 6, no. 2, pp. 644–652, Apr. 2015.
- [13] M. Miyatake, M. Veerachary, F. Toriumi, N. Fujii, and H. Ko, "Maximum power point tracking of multiple photovoltaic arrays: A PSO approach," *IEEE Trans. Aerosp. Electron. Syst.*, vol. 47, no. 1, pp. 367–380, Jan. 2011.
- [14] S. R. Chowdhury and H. Saha, "Maximum power point tracking of par-tially shaded solar photovoltaic arrays," *Solar Energy Mater. Solar Cells*, vol. 94, pp. 1441–1447, Jan. 2010.
- [15] V. N. Lal and S. N. Singh, "Modified particle swarm optimisation-based maximum power point tracking controller for single-stage utility-scale photovoltaic system with reactive power injection capability," *IET Renew-able Power Gener.*, vol. 10, no. 7, pp. 899–907, Jul. 2016.
- [16] K. Ishaque and Z. Salam, "A deterministic particle swarm optimization maximum power point tracker for photovoltaic system under partial shad-ing condition," *IEEE Trans. Ind. Electron.*, vol. 60, no. 8, pp. 3195–3206, Aug. 2013.
- [17] K. Ishaque, Z. Salam, M. Amjad, and S. Mekhilef, "An improved particle swarm optimization (PSO)-based MPPT for PV with reduced steady-state oscillation," *IEEE Trans. Power Electron.*, vol. 27, no. 8, pp. 3627–3638, Aug. 2012.
- [18] R. Koad, A. F. Zobia, and A. El Shahat, "A novel MPPT algorithm based on particle swarm optimisation for photovoltaic systems," *IEEE Trans. Sustain. Energy*, 2016.
- [19] C. Manickam, G. R. Raman, G. P. Raman, S. I. Ganesan, and C. Nagamani, "A hybrid algorithm for tracking of global MPP based on perturb and observe and particle swarm optimization with reduced power oscillation in string inverters," *IEEE Trans. Ind. Electron.*, vol. 63, no. 10, pp. 6097–6106, Oct. 2016.

- [20] M. Seyedmahmoudian *et al.*, "Simulation and hardware implementation of new maximum power point tracking technique for partially shaded PV system using hybrid DEPSO method," *IEEE Trans. Sustain. Energy*, vol. 6, no. 3, pp. 850–862, Jul. 2015.
- [21] D. Teshome, C. H. Lee, Y. W. Lin, and K. L. Lian, "A modified firefly algorithm for photovoltaic maximum power point tracking control under partial shading," *IEEE J. Emerg. Sel. Topics Power Electron.*, 2016.
- [22] H. S. Sahu and S. K. Nayak, "Numerical approach to estimate the maximum power point of a photovoltaic array," *IET Gener., Transm. Distrib.*, vol. 10, no. 11, pp. 2670–2680, Apr. 2016.
- [23] E. Nery Chaves, J. Henrique Reis, E. A. Alves Coelho, L. C. Gomes De Freitas, J. B. Vieira Junior, and L. C. Freitas, "Simulated Annealing-MPPT in partially shaded PV systems," *IEEE Latin Amer. Trans.*, vol. 14, no. 1, pp. 235–241, Jan. 2016.
- [24] S. Lyden and M. E. Haque, "A simulated annealing global maximum power point tracking approach for PV modules under partial shading conditions," *IEEE Trans. Power Electron.*, vol. 31, no. 6, pp. 4171–4181, Jun. 2016.
- [25] S. Mirjalili, S. M. Mirjalili, and A. Lewis, "Grey wolf optimizer," *Adv. Eng. Softw.*, vol. 69, pp. 46–61, Jan. 2014.
- [26] A. Zhu, C. Xu, Z. Li, J. Wu, and Z. Liu, "Hybridizing grey wolf optimization with differential evolution for global optimization and test scheduling for 3D stacked SoC," *J. Syst. Eng. Electron.*, vol. 26, no. 2, pp. 317–328, Apr. 2015.
- [27] S. Mirjalili and A. Lewis, "The whale optimization algorithm," *Adv. Eng. Softw.*, vol. 95, pp. 51–67, Jan. 2016.
- [28] K. V. Price, R. M. Storn, and J. A. Lampinen, "Differential Evolution: A Practical Approach to Global Optimization," Berlin, Germany: Springer-Verlag, 2005.
- [29] A. P. Engelbrecht, "Differential Evolution," *Computational Intelligence: An Introduction*, 2nd ed. Hoboken, NJ, USA: Wiley 2007, ch. 13, pp. 237–260.
- [30] M. G. Villalva, J. R. Gazoli, and E. R. Filho, "Comprehensive approach to modeling and simulation of photovoltaic arrays," *IEEE Trans. Power Electron.*, vol. 24, no. 5, pp. 1198–1208, May 2009.

